Separable solutions to non-linear anisotropic diffusion equation in elliptic coordinates

K. Tretiakova[1] and Y. Nec[1]

[1] Department of Mathematics and Statistics, Thompson Rivers University, British Columbia, Canada

Abstract

Two- and three-dimensional exact solutions of the non-linear diffusion equation are proved to exist in elliptic coordinates subject to an arbitrary piecewise constant azimuthal anisotropy. Degrees of freedom traditionally used to satisfy boundary conditions are instead employed to ensure continuity and conservation of mass across contiguity surfaces between subdomains of distinct diffusivities. Not all degrees of freedom are exhausted thereby and conditions are given for the inclusion of higher harmonics. Degrees of freedom associated with one isotropic subdomain are always available to satisfy boundary conditions. The second harmonic is pivotal in the solution construction as well as identification of partial symmetries in the domain partition. The anisotropy gives rise to an unconventional mixed type critical point that combines saddle and node-like characteristics.

Keywords: non-linear diffusion, anisotropy, elliptic coordinates

MSC subjects: 35C05, 35G60, 76R50, 76S05

1 Background

The steady non-linear diffusion equation

$$\nabla \cdot \Big(- K u^{\gamma-1} \nabla u \Big) = C \tag{1.1}$$

emerges in numerous contexts in physics and engineering. The unknown function u denotes the diffusing entity, K is the diffusivity, and C – the source or sink. The non-linearity parameter $\gamma \neq 0$ is constant. Whilst isotropic and axially symmetric solutions are elementary [1], the complexity of many natural or man-made media requires a more realistic description. The studies seeking to break the symmetry via a generalisation to elliptic domains – be it of solid or virtual boundaries – are rare, and despite a series of preluding simplifications, eventuate in the usage of finite element methods [2, 3, 4]. Modelling anisotropic transport is of interest in large scale applications, such as diffusion in construction materials [5] and subsurface flows near oil reservoirs [6, 7] or aquifers [8]. As the permeability of these media cannot be controlled at will, analytical solutions supporting a flexible spatial anisotropy dependence are of value, doubly so if the constraint due to the idealised circular cross-section geometry can be relaxed.

The isotropic homogeneous version of (1.1) is equivalent to the Laplace's equation for u^γ and thus separable in 13 coordinate systems [9]. The separability of Laplace's equation had been studied by many famous mathematicians, resulting in the definition of several families of special functions. A recent discovery of an expansive class of solutions with arbitrary piecewise constant azimuthal anisotropy in polar [10, 11] and spherical [12] coordinates prompts the question of existence in other coordinate systems. The intricacy of connection between the separability of Laplace's equation and existence of anisotropic solutions is a crucial point that escaped classical works. This study is a step in an effort to delineate the conditions under which the anisotropic solutions persist in curvilinear orthogonal coordinate systems. The mainstay feature underpinning these solutions is that one coordinate traces closed orbits in the Cartesian space. In polar and spherical coordinates these are circles, conducing a further question whether existence hinges on axial symmetry. The aim of the current contribution is to answer this fundamental question in the negative by constructing anisotropic solutions in the elliptic coordinate system. This system, whilst possessing the requisite periodic orbits, lacks the axial symmetry inherent to polar and spherical framework.

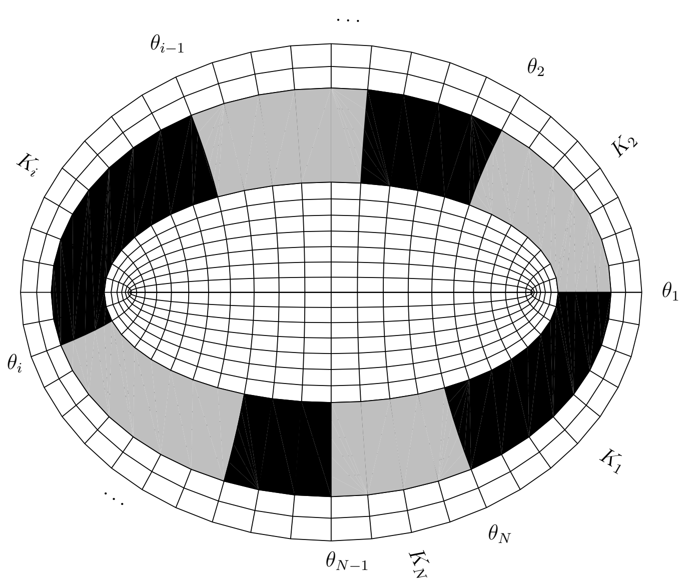

Figure 1: Anisotropic configuration $\{\theta_i\}$ with distinct diffusivities $\{K_i\}$, $i = \{1, \ldots, N\}$, in the elliptic coordinate system.

In a generic system of curvilinear orthogonal coordinates (ξ_1, ξ_2, ξ_3) the i-th component of the gradient of a scalar function u is

$$(\nabla u)_i = \frac{1}{h_i}\frac{\partial u}{\partial \xi_i} \tag{1.2a}$$

and the divergence of a vector function $\mathbf{f} = (f_1, f_2, f_3)$ is

$$\nabla \cdot \mathbf{f} = \frac{1}{h_1 h_2 h_3}\left\{\frac{\partial}{\partial \xi_1}\big(h_2 h_3 f_1\big) + \frac{\partial}{\partial \xi_2}\big(h_1 h_3 f_2\big) + \frac{\partial}{\partial \xi_3}\big(h_1 h_2 f_3\big)\right\}, \tag{1.2b}$$

where the scale factors h_i, $i = \{1, 2, 3\}$, are defined by the following relation between the Cartesian system (x, y, z) and the new system:

$$h_i^2 = \left(\frac{\partial x}{\partial \xi_i}\right)^2 + \left(\frac{\partial y}{\partial \xi_i}\right)^2 + \left(\frac{\partial z}{\partial \xi_i}\right)^2. \tag{1.2c}$$

The elliptic cylinder system (ξ, θ, ζ) is defined by

$$x = f\cosh\xi\cos\theta, \quad y = f\sinh\xi\sin\theta, \quad z = \zeta, \tag{1.3a}$$

where $\xi > 0$ measures distance along confocal hyperbolae with foci on the x-axis at $(\pm f, 0, 0)$, and $0 \leqslant \theta < 2\pi$ is an elliptic arc length (see figure 1). Definition (1.2c) permits to define $h := h_1 = h_2$ and yields

$$h^2 = \frac{1}{2}f^2\Big(\cosh(2\xi) - \cos(2\theta)\Big), \quad h_3 = 1, \tag{1.3b}$$

wherewith equation (1.1) becomes

$$\frac{\partial}{\partial\xi}\left(K\frac{\partial u^\gamma}{\partial\xi}\right)+\frac{\partial}{\partial\theta}\left(K\frac{\partial u^\gamma}{\partial\theta}\right)+\frac{\partial}{\partial\zeta}\left(Kh^2\frac{\partial u^\gamma}{\partial\zeta}\right)=-\gamma Ch^2. \tag{1.4}$$

Consider an elliptic annulus $\xi_{\text{in}} \leqslant \xi \leqslant \xi_{\text{ex}}$ divided into an arbitrary number of subdomains by angles $\{\theta_i\}_{i=1}^N$ such that $K_i \neq K_{i+1}$ for any $1 \leqslant i \leqslant N$. The index $i+1$ is wrapped back to 1 for $i = N$, since the N-th and first subdomains are contiguous. By the conceptual similarity to the polar geometry, the subdomains might be referred to as sectors. The source C is taken constant throughout: it is shown hereunder that a problem with a piecewise constant C is equivalent to one with a uniform C and redefined set $\{K_i\}_{i=1}^N$.

The function u must be continuous throughout the domain, i.e.

$$u\Big|_{\theta_i^-}=u\Big|_{\theta_i^+},\quad 1\leqslant i\leqslant N. \tag{1.5a}$$

Since K is not constant, the condition of conservation of angular flux across the contiguity surfaces $\theta = \theta_i$ is obtained by integrating (1.4) along an infinitesimal arc $(\theta_i - \varepsilon, \theta_i + \varepsilon)$ and taking the limit $\varepsilon \longrightarrow 0$:

$$\left(K\frac{\partial u}{\partial\theta}\right)_{\theta_i^-}=\left(K\frac{\partial u}{\partial\theta}\right)_{\theta_i^+},\quad 1\leqslant i\leqslant N. \tag{1.5b}$$

Conditions (1.5) are instrumental in constructing a valid anisotropic solution, and are formally identical to the polar and spherical settings, only the meaning encoded by the coordinate θ here is new.

2 Anisotropic solution existence

(a) Two-dimensional flow

Within each isotropic sector the diffusivity K is constant and thus can be factored out of the divergence operator in (1.4). Begin with a two-dimensional version of (1.4) by setting $\partial_\zeta \equiv 0$ and seeking a separated solution

$$u_i^\gamma(\xi,\theta)=-\frac{\gamma f^2}{8K_i}\,C\Big(\cosh(2\xi)+\cos(2\theta)\Big)+A(\xi)B(\theta). \tag{2.1}$$

The functions A and B satisfy the ordinary differential equations

$$A''-\alpha^2A=0\quad\text{and}\quad B''+\alpha^2B=0, \tag{2.2}$$

where α is the separation constant. Since the scale factor h is periodic in θ, demanding periodicity for u will also ensure periodicity for the flux that is proportional to ∇u. Thus enforcing $B(\theta) = B(\theta + 2\pi)$ yields $\alpha = m$, $m \in \mathbb{Z}$. When $\alpha = 0$, the eigenfunctions are given by $B_o \equiv 1$ and $A_o = a_o + b_o\xi$. All other values of m result in $B_m \in \operatorname{span}\Big\{\sin(m\theta), \cos(m\theta)\Big\}$ together with $A_m \in \operatorname{span}\Big\{\exp(m\xi), \exp(-m\xi)\Big\}$. This basis for the function A_m allows for an elegant separation of components that decay or blow up as $\xi \longrightarrow \infty$. The isotropic solution within sector i is then written as

$$u_i^\gamma=\frac{\gamma f^2}{8K_i}\Bigg\{-C\cosh(2\xi)-C\cos(2\theta)+a_o^{(i)}+b_o^{(i)}\xi+ \tag{2.3}$$

$$\sum_{m=1}^{\infty}\left(\mathrm{e}^{m\xi}\Big(a_m^{(i)}\sin(m\theta)+b_m^{(i)}\cos(m\theta)\Big)+\mathrm{e}^{-m\xi}\Big(\alpha_m^{(i)}\sin(m\theta)+\beta_m^{(i)}\cos(m\theta)\Big)\right)\Bigg\},$$

where $a_m^{(i)}, b_m^{(i)}, \alpha_m^{(i)}$ and $\beta_m^{(i)}$ are constants to be determined. Form (2.3) allows to set $C = 0$ without affecting the analysis hereinafter and shows that possibly distinct values of C in different sectors might be redefined to equal a single uniform value by utilising the ratios $C \big/ K_i$.

Theorem 2.1 *Let k_i be the ratios of diffusivities in adjacent sectors: $k_i = K_i \big/ K_{i+1}$ $\forall 1 \leqslant i \leqslant N-1$ and $k_N = K_N \big/ K_1$. Furthermore, if $C \neq 0$, suppose the configuration as defined by $\{\theta_i\}_{i=1}^N$ and $\{k_i\}_{i=1}^N$ satisfies the compatibility condition*

$$k_1 \cdot \ \ldots \ \cdot k_{N-1}(1-k_N)\cos(2\theta_N) + \ldots + k_1(1-k_2)\cos(2\theta_2) + (1-k_1)\cos(2\theta_1) = 0. \tag{2.4}$$

Then the anisotropic, 2π-periodic solution to (1.4) in the domain $\Big\{(\xi,\theta)\,\Big|\,\xi_{in} \leqslant \xi \leqslant \xi_{ex},\ 0 \leqslant \theta < 2\pi\Big\}$ exists if and only if the following (almost) block bidiagonal linear system possesses a non-trivial solution for $m = 2$:

$$\mathfrak{C}^{(m)}\mathbf{c}_m = \mathbf{r}, \tag{2.5a}$$

where the vector $\mathbf{c}_m$ stands for $\Big(a_m^{(1)},\ b_m^{(1)},\ \cdots,\ a_m^{(N)},\ b_m^{(N)}\Big)^T$ and $\Big(\alpha_m^{(1)},\ \beta_m^{(1)},\ \cdots,\ \alpha_m^{(N)},\ \beta_m^{(N)}\Big)^T$, the matrix $\mathfrak{C}^{(m)}$ is defined as

$$\mathfrak{C}^{(m)} = \begin{pmatrix} \mathfrak{A}_1^{(m)} & \mathfrak{B}_1^{(m)} & & & \\ & \mathfrak{A}_2^{(m)} & \mathfrak{B}_2^{(m)} & & \\ & & \ddots & \ddots & \\ & & & \mathfrak{A}_{N-1}^{(m)} & \mathfrak{B}_{N-1}^{(m)} \\ \mathfrak{B}_N^{(m)} & & & & \mathfrak{A}_N^{(m)} \end{pmatrix}, \tag{2.5b}$$

with the block matrices given by

$$\mathfrak{A}_i^{(m)} = \begin{pmatrix} \sin(m\theta_i) & \cos(m\theta_i) \\ \cos(m\theta_i) & -\sin(m\theta_i) \end{pmatrix}, \qquad \mathfrak{B}_i^{(m)} = \begin{pmatrix} -k_i\sin(m\theta_i) & -k_i\cos(m\theta_i) \\ -\cos(m\theta_i) & \sin(m\theta_i) \end{pmatrix}. \tag{2.5c}$$

System (2.5a) is homogeneous if $m \neq 2$, whereas for $m = 2$ the right-hand side vector $\mathbf{r}$ equals

$$\mathbf{r} = \frac{C}{2}\Big(1-k_1,\ 0,\ \cdots,\ 1-k_N,\ 0\Big)^T. \tag{2.5d}$$

PROOF Implementing the continuity conditions (1.5) for a pair of adjacent sectors i and $i+1$ separated by the contiguity curve θ_i for $m = 1$ or any $m > 2$ gives

$$\Big(\mathfrak{A}_i^{(m)} \quad \mathfrak{B}_i^{(m)}\Big)\begin{pmatrix} a_m^{(i)} \\ b_m^{(i)} \\ a_m^{(i+1)} \\ b_m^{(i+1)} \end{pmatrix} = \begin{pmatrix} 0 \\ 0 \end{pmatrix}. \tag{2.6a}$$

For $m = 2$ the left-hand side is identical, but the right-hand side is inhomogeneous if $C \neq 0$:

$$\Big(\mathfrak{A}_i^{(2)} \quad \mathfrak{B}_i^{(2)}\Big)\begin{pmatrix} a_2^{(i)} \\ b_2^{(i)} \\ a_2^{(i+1)} \\ b_2^{(i+1)} \end{pmatrix} = \frac{C}{2}\begin{pmatrix} 1-k_i \\ 0 \end{pmatrix}. \tag{2.6b}$$

For the coefficients $\alpha_m^{(i)}$ and $\beta_m^{(i)}$ identical equations ensue. Collecting the systems for all θ_i gives (2.5). Because (2.5) is inhomogeneous for $m = 2$, unless a non-trivial solution $\mathbf{c}_m$ exists, there will be no solution to (1.4). In other words, either $\det \mathfrak{C}^{(2)} \neq 0$, or if $\det \mathfrak{C}^{(2)} = 0$, the right-hand side vector $\mathbf{r}$ must be orthogonal to the null space of ${\mathfrak{C}^{(m)}}^{\mathrm{T}}$. If $\det \mathfrak{C}^{(m)} \neq 0$ for $m = 1$ or any $m > 2$, the respective coefficients $\mathbf{c}_m$ vanish, however that does not thwart the existence of a solution to (1.4). If $\det \mathfrak{C}^{(m)} = 0$, a non-trivial $\mathbf{c}_m$ will introduce harmonics of frequency m into (2.3). In light of the above, $m = 2$ gives $a_2^{(i)} = \alpha_2^{(i)}$ and $b_2^{(i)} = \beta_2^{(i)}$ for all i. For all other m if $\det \mathfrak{C}^{(m)} = 0$, no such pairwise equality needs to be enforced.

The harmonic $m = 0$ requires a separate treatment. Implementing (1.5a) for the coefficients $b_o^{(i)}$ in adjacent sectors gives $b_o^{(i)} = k_i b_o^{(i+1)}$. This is a linear homogeneous system in N unknowns $b_o^{(i)}$. Writing this relation for all $1 \leqslant i \leqslant N$ leads to

$$b_o^{(1)} = \prod_{j=1}^{N-1} k_j \; b_o^{(N)} = \prod_{j=1}^{N} k_j \; b_o^{(1)}. \tag{2.7}$$

Since $\prod\limits_{j=1}^{N} k_j = 1$ is an identity, the linear system is soluble with a single degree of freedom: $b_o^{(i)} = b_o^{(1)} \Big/ \prod\limits_{j=1}^{i-1} k_j$. An identical argument for the coefficients $a_o^{(i)}$ creates an inhomogeneous system: $a_o^{(i)} = k_i a_o^{(i+1)} - C(k_i - 1)\cos(2\theta_i)$ that is only soluble if $C = 0$ or if (2.4) holds. ■

Remark 2.1 *System (2.5) and concomitant solvability conditions have appeared in the analysis of anisotropic diffusion in polar and spherical coordinates [11, 12], but without the compatibility condition (2.4). The elliptic coordinate system is the first, where this condition emerges. The conjecture on its degeneracy in axially symmetric geometries is a topic of future studies.*

An example of the complexity of topological terrain supported by (2.3) is given in figure 2. The degrees of freedom $a_o^{(i)}$, $b_o^{(i)}$ might be determined via boundary conditions for the transversal (ξ-direction) flow in one sector. If, for instance, the desired range of ξ is $\xi_{\mathrm{in}} \leqslant \xi \leqslant \xi_{\mathrm{ex}}$, define the transversal part as

$$u_{\mathrm{t}}^{(i)} = \left\{ \frac{\gamma f^2}{8K_i} \Big(-C\cosh(2\xi) + a_o^{(i)} + b_o^{(i)}\xi \Big) \right\}^{1/\gamma}. \tag{2.8}$$

Then for a given generation rate C and permeability K_i in one chosen sector i it is possible to set $a_o^{(i)}$, $b_o^{(i)}$ to satisfy given values $u_{\mathrm{t}}^{(i)}(\xi_{\mathrm{in}}) = u_{\mathrm{in}}^{(i)}$ and $u_{\mathrm{t}}^{(i)}(\xi_{\mathrm{ex}}) = u_{\mathrm{ex}}^{(i)}$. These values ultimately bear on the ability to construct a real solution when u represents a positive physical quantity and γ is even. Sufficiently large free coefficients in the transversal part allow for a real solution with larger oscillatory components in (2.3). For high harmonics the magnitude of the coefficients $\alpha_m^{(i)}$ and $\beta_m^{(i)}$ might need to exceed significantly that of $a_m^{(i)}$ and $b_m^{(i)}$ for their contribution to be tangible due to the decaying exponential factor $\exp(-m\xi)$. In general, all coefficients in a single sector might be determined by expanding a desired boundary condition in the function basis set by (2.3). The coefficients in the other sectors follow by the continuity conditions (1.5).

Note the peculiar shape of contours in the vicinity of the fixed point marked by a diamond on the contiguity curve corresponding to θ_1: their appearance does not resemble any of the local contour shape characteristic of conventional critical points. This point is positioned on a boundary between two subdomains of distinct diffusivities. When this happens, condition (1.5b) is satisfied because the tangential derivative u_θ vanishes, i.e. at this point u_θ is continuous across the contiguity curve. The contours on the two sides depend on the topological terrain in each sector, and might well correspond to critical points of different types, creating a mixed type fixed point. This occurrence is further discussed in §4.

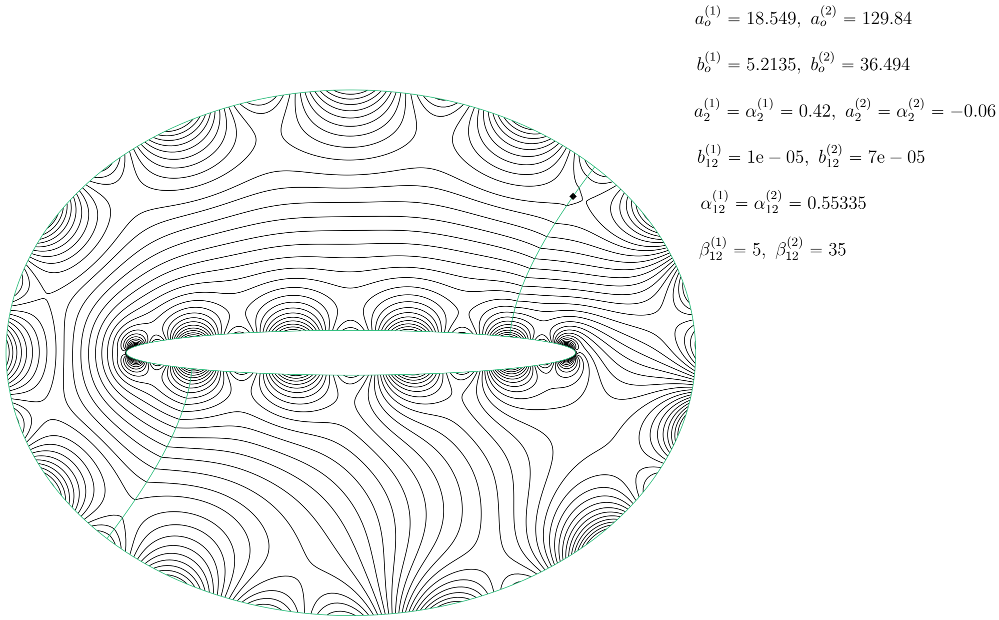

Figure 2: Isocontour map of (2.3) with $m = 2$ and $m = 12$: $K_1 = 1$, $K_2 = 7$, $\theta_1 = \pi/4$, $\theta_2 = 5\pi/4$ (green / grey curves), $C = 0.2$, $\gamma = 2$, $f = 1$, $\xi_{\text{in}} = 0.1$, $\xi_{\text{ex}} = 1$, $u_{\text{in}}^{(1)} = 0.95$, $u_{\text{ex}}^{(1)} = 1$; coefficient values as stated (given to 5 significant figures); contour level linearly distributed (density corresponds to gradient); diamond on θ_1 curve marks a mixed type fixed point.

(b) Tridimensional flow

Seeking a separated solution

$$u_i^{\gamma}(\xi, \theta, \zeta) = -\frac{\gamma f^2}{8K_i} C\Big(\cosh(2\xi) + \cos(2\theta)\Big) + A(\xi)B(\theta)Z(\zeta) \tag{2.9}$$

within each isotropic sector gives the ordinary differential equations

$$A'' + \Big(-a + 2q\cosh(2\xi)\Big)A = 0, \quad 2q := \frac{1}{2}\lambda f^2 \tag{2.10a}$$

$$B'' + \Big(a - 2q\cos(2\theta)\Big)B = 0, \tag{2.10b}$$

$$Z'' - \lambda Z = 0, \tag{2.10c}$$

where λ and a are separation constants. The solutions to (2.10a) and (2.10b) depend on the sign of λ and thus on the boundary conditions imposed for Z. The simpler possibility is that (2.10c) holds on a half line, so that $\lambda \geqslant 0$. Suppose first $\lambda > 0$. Then $q > 0$ and an infinite sequence of eigenvalues a in (2.10b) generates periodic solutions via the Mathieu functions of the first kind, also known as sine-elliptic and cosine-elliptic functions [13, **8.62**]:

$$\mathrm{ce}_{2\mathfrak{m}}(\theta; q) = \sum_{r=0}^{\infty} A_{2r}^{(2\mathfrak{m})} \cos(2r\theta), \quad \mathrm{ce}_{2\mathfrak{m}+1}(\theta; q) = \sum_{r=0}^{\infty} A_{2r+1}^{(2\mathfrak{m}+1)} \cos((2r+1)\theta), \tag{2.11a}$$

$$\mathrm{se}_{2\mathfrak{m}+1}(\theta;q)=\sum_{r=0}^{\infty}B_{2r+1}^{(2\mathfrak{m}+1)}\sin((2r+1)\theta),\quad \mathrm{se}_{2\mathfrak{m}+2}(\theta;q)=\sum_{r=0}^{\infty}B_{2r+2}^{(2\mathfrak{m}+2)}\sin((2r+2)\theta).$$

The series coefficients $A_r^{(\mathfrak{m})}$ and $B_r^{(\mathfrak{m})}$ are computed separately for even and odd $\mathfrak{m}$. The corresponding solutions to (2.10a) are the associated Mathieu functions of the first kind [13, **8.63**]:

$$\mathrm{Ce}_{2\mathfrak{m}}(\xi;q)=\sum_{r=0}^{\infty}A_{2r}^{(2\mathfrak{m})}\cosh(2r\xi),\quad \mathrm{Ce}_{2\mathfrak{m}+1}(\xi;q)=\sum_{r=0}^{\infty}A_{2r+1}^{(2\mathfrak{m}+1)}\cosh((2r+1)\xi), \tag{2.11b}$$

$$\mathrm{Se}_{2\mathfrak{m}+1}(\xi;q)=\sum_{r=0}^{\infty}B_{2r+1}^{(2\mathfrak{m}+1)}\sinh((2r+1)\xi),\quad \mathrm{Se}_{2\mathfrak{m}+2}(\xi;q)=\sum_{r=0}^{\infty}B_{2r+2}^{(2\mathfrak{m}+2)}\sinh((2r+2)\xi).$$

The case $\lambda=0$ gives $Z(\zeta)=\tilde{a}_o+\tilde{b}_o\zeta$. The only bounded solution is then $Z_o\equiv 1$, and the functions A and B coincide with the two-dimensional solution. Combining all of the above yields

$$u_i^\gamma\Big|_{3\mathrm{D}}=u_i^\gamma\Big|_{2\mathrm{D}}+\frac{\gamma f^2}{8K_i}\sum_{n=1}^{\infty}\sum_{\mathfrak{m}=1}^{\infty}Z_n(\zeta)\Bigg\{\Big(a_{n\mathfrak{m}}^{(i)}\,\mathrm{se}_{\mathfrak{m}}(\theta)+b_{n\mathfrak{m}}^{(i)}\,\mathrm{ce}_{\mathfrak{m}}(\theta)\Big)\,\mathrm{Ce}_{\mathfrak{m}}(\xi)+ \tag{2.12}$$

$$\Big(\alpha_{n\mathfrak{m}}^{(i)}\,\mathrm{se}_{\mathfrak{m}}(\theta)+\beta_{n\mathfrak{m}}^{(i)}\,\mathrm{ce}_{\mathfrak{m}}(\theta)\Big)\,\mathrm{Se}_{\mathfrak{m}}(\xi)\Bigg\},$$

where Z_n is the sequence of eigenfunctions generated by (2.10c) and $u_i^\gamma\Big|_{2\mathrm{D}}$ is given by (2.3).

The slightly more complicated possibility is when (2.10c) is to form a regular Sturm-Liouville problem on a finite interval $0<\zeta<\zeta_o$ for some $\zeta_o>0$, resulting in $\lambda\leqslant 0$. The identity $\cos\Big(2(\pi/2-\theta)\Big)=-\cos(2\theta)$ allows to arrange the sign in (2.10b) to give the same form as before with respective solutions $\mathrm{ce}_{\mathfrak{m}}(\pi/2-\theta;q)$, $\mathrm{se}_{\mathfrak{m}}(\pi/2-\theta;q)$. The variable transformation $\xi\longmapsto\xi+\pi\imath/2$, where $\imath$ is the imaginary unit, yields the desired signs in (2.10a), but eventuates in a formally complex basis $\mathrm{Ce}_{\mathfrak{m}}(\xi+\pi\imath/2;q)$, $\mathrm{Se}_{\mathfrak{m}}(\xi+\pi\imath/2;q)$. In reality since definitions (2.11b) use either even or odd frequencies, the functions of the transformed variable will have the same series coefficients, but with alternating signs. The multiple of $\imath$ that appears for the odd pair is removed due to linearity in order to have a real solution. The fact that the odd $\mathrm{Ce}_{\mathfrak{m}}$ and $\mathrm{Se}_{\mathfrak{m}}$ swap, is equivalent to reshuffling the coefficients within the double sum in (2.12) and thus might be disregarded. The next step is to identify the relationship between the coefficients $a_{n\mathfrak{m}}^{(i)}$, $b_{n\mathfrak{m}}^{(i)}$, $\alpha_{n\mathfrak{m}}^{(i)}$ and $\beta_{n\mathfrak{m}}^{(i)}$ entailing a valid anisotropic solution.

Remark 2.2 *A fundamental disparity between the functions* $\mathrm{se}_{\mathfrak{m}}(\theta),\mathrm{ce}_{\mathfrak{m}}(\theta)$ *and elementary* $\sin(m\theta),\cos(m\theta)$ *is that the latter form a pair of independent solutions to a differential equation with a common eigenvalue that depends on* m*. By contrast,* $\mathrm{se}_{\mathfrak{m}}$*,* $\mathrm{ce}_{\mathfrak{m}}$ *are mere labels, each constituting a solution to a distinct differential equation with* $\mathfrak{m}$ *denoting the placement in a sequence of eigenvalues. The sequence of eigenvalues and eigenfunctions solving the Sturm-Liouville problem (2.10b) with periodic boundary conditions comprises four interlaced sequences given by (2.11a).*

Remark 2.3 *The linear combination of the type used in (2.12) should generally include the index* $m=0$*, i.e. terms of the form* $b_{n0}^{(i)}Z_n(\zeta)\,\mathrm{ce}_0(\theta)\,\mathrm{Ce}_0(\xi)$*. A valid anisotropic solution must satisfy the continuity conditions (1.5), which result in the conclusion that* $b_{n0}^{(i)}=0$ *for all* i *and* n*.*

Corollary 2.1 *Suppose the conditions of theorem 2.1 hold. Then there exists an anisotropic, 2π-periodic solution to (1.4) in the domain $\left\{(\xi,\theta,\zeta)\,\middle|\,\xi_{in} \leqslant \xi \leqslant \xi_{ex},\ 0 \leqslant \theta < 2\pi, \zeta \in I\right\}$, where $I = [\zeta_o,\ \infty)$ for some real ζ_o, or $I = [0,\ \zeta_o]$ with some $\zeta_o > 0$. The solution includes elliptic harmonics $\mathfrak{m} \geqslant 1$ if and only if*

$$\det \mathfrak{C}^{(\mathfrak{m})} = \det \begin{pmatrix} \mathfrak{A}_1^{(\mathfrak{m})} & \mathfrak{B}_1^{(\mathfrak{m})} & & & & \\ & \mathfrak{A}_2^{(\mathfrak{m})} & \mathfrak{B}_2^{(\mathfrak{m})} & & & \\ & & \ddots & \ddots & & \\ & & & \mathfrak{A}_{N-1}^{(\mathfrak{m})} & \mathfrak{B}_{N-1}^{(\mathfrak{m})} \\ \mathfrak{B}_N^{(\mathfrak{m})} & & & & \mathfrak{A}_N^{(\mathfrak{m})} \end{pmatrix} = 0, \tag{2.13a}$$

where

$$\mathfrak{A}_i^{(\mathfrak{m})} = \begin{pmatrix} \mathrm{se}_{\mathfrak{m}}(\theta_i) & \mathrm{ce}_{\mathfrak{m}}(\theta_i) \\ \mathrm{se}'_{\mathfrak{m}}(\theta_i) & \mathrm{ce}'_{\mathfrak{m}}(\theta_i) \end{pmatrix}, \qquad \mathfrak{B}_i^{(\mathfrak{m})} = -\begin{pmatrix} k_i\,\mathrm{se}_{\mathfrak{m}}(\theta_i) & k_i\,\mathrm{ce}_{\mathfrak{m}}(\theta_i) \\ \mathrm{se}'_{\mathfrak{m}}(\theta_i) & \mathrm{ce}'_{\mathfrak{m}}(\theta_i) \end{pmatrix}. \tag{2.13b}$$

Proof The two-dimensional part in (2.12) satisfies conditions (1.5) via theorem 2.1. Imposing (1.5) for the tridimensional part of (2.12) makes it obvious that the choice of bases for $A(\xi)$ and $Z(\zeta)$ in (2.12) has no bearing on the ability to satisfy (1.5). Thus the result will hold for all domain types above that without loss of generality encompass all bounded solutions accorded by (2.10c). The adjacency structure of (1.5) results in a system identical in form to (2.5), homogeneous for all combinations of m and n in (2.12) for coefficients of type $a_{nm}^{(i)}, b_{nm}^{(i)}$ and $\alpha_{nm}^{(i)}, \beta_{nm}^{(i)}$. The only difference is that the derivatives of $\mathrm{se}_{\mathfrak{m}}(\theta)$ and $\mathrm{ce}_{\mathfrak{m}}(\theta)$ cannot be expressed via the same functions as elegantly as with the elementary sine and cosine functions. Instead the derivatives are obtained by an element-wise differentiation of series (2.11a). Since the system is homogeneous, the only option to obtain a non-trivial solution is via a non-zero determinant. ∎

The coefficients in the series defining the Mathieu functions (2.11a) and (2.11b) are given by a second order recurrence relations that form an infinite eigenvalue-eigenvector system, distinct for even and odd $\mathfrak{m}$ values and $\mathrm{se}_{\mathfrak{m}}$ and $\mathrm{ce}_{\mathfrak{m}}$ functions [13, **8.62**]. When sorted in ascending order, the $\mathfrak{m}$-th eigenvalue corresponds to the $\mathfrak{m}$-th value in the Sturm-Liouville sequence of the separation constant a in (2.10b). The $\mathfrak{m}$-th eigenvector gives the coefficients $A_r^{(\mathfrak{m})}$ and $B_r^{(\mathfrak{m})}$ for $\mathrm{ce}_{\mathfrak{m}}$ or $\mathrm{se}_{\mathfrak{m}}$ series. To compute the coefficients in practice one constructs ever increasing matrices and calculates the corresponding eigenvalues and eigenvectors. The series is summed simultaneously for all $0 \leqslant \theta < 2\pi$ and function normalised so as to have $\int_0^{2\pi} B^2(\theta)d\theta = \pi$. Thus the source of error is twofold: the truncation of the infinite matrix and the error inherent to the algorithm computing eigenvalues and eigenvectors. MATLAB and Octave offer no built-in routines to compute the Mathieu functions, but routines to solve eigenvalue problems are readily available. All results involving Mathieu functions were computed using Octave [14] up to a tolerance of $\epsilon = 10^{-12}$ and $\epsilon = 10^{-8}$ for 2D and 3D flow respectively: the eigensystem size is doubled every iteration and only the first half of the coefficients is used for series summation (since coefficients in positions close to the end of the vector are not expected to be accurate) until the maximal difference between the function thus obtained and previous iteration is less than ϵ. There is no user control of accuracy of output returned by the built-in function `eig` computing the eigenvalues and eigenvectors. Therefore the above tolerance is the best that is reasonably achievable for a wide range of q and $\mathfrak{m}$ without full control of the second source of error.

Hereinafter the harmonics ensuing by (2.5) and (2.13) are respectively referred to as *basic* and *elliptic*, and denoted by m and $\mathfrak{m}$ to avoid confusion. The theory governing the inclusion of basic harmonics in both (2.3) and (2.12) is coincident with that of polar and spherical coordinates, albeit the flow itself is completely different. The elliptic harmonics are unique to the current setting and hence the focus of the analysis below.

3 Compatibility and singular manifolds

The singular manifold is defined as all layouts $\{\theta_i\}_{i=1}^N$ and concomitant diffusivities $\{K_i\}_{i=1}^N$, for which $\det \mathfrak{C}^{(\mathfrak{m})} = 0$. In order to prove several instructive characteristics it is useful to employ the LU decomposition of $\mathfrak{C}^{(\mathfrak{m})}$:

$$\mathfrak{C}^{(\mathfrak{m})} = \begin{pmatrix} \mathrm{I}_{2\times2} & & & & \\ & \mathrm{I}_{2\times2} & & & \\ & & \ddots & & \\ & & & \mathrm{I}_{2\times2} & \\ \mathrm{L}_{N,1} & \cdots & & \mathrm{L}_{N,N-1} & \mathrm{I}_{2\times2} \end{pmatrix} \begin{pmatrix} \mathfrak{A}_1^{(\mathfrak{m})} & \mathfrak{B}_1^{(\mathfrak{m})} & & & \\ & \mathfrak{A}_2^{(\mathfrak{m})} & \mathfrak{B}_2^{(\mathfrak{m})} & & \\ & \ddots & \ddots & & \\ & & & \mathfrak{A}_{N-1}^{(\mathfrak{m})} & \mathfrak{B}_{N-1}^{(\mathfrak{m})} \\ & & & & \mathrm{U}_{NN} \end{pmatrix}, \tag{3.1a}$$

where $\mathfrak{A}_i^{(\mathfrak{m})}$, $\mathfrak{B}_i^{(\mathfrak{m})}$ are defined in (2.13b) and

$$\mathrm{U}_{NN} = \mathfrak{A}_N^{(\mathfrak{m})} - (-1)^N \mathfrak{B}_N^{(\mathfrak{m})} \mathfrak{A}_1^{(\mathfrak{m})^{-1}} \mathfrak{B}_1^{(\mathfrak{m})} \times \ldots \times \mathfrak{A}_{N-1}^{(\mathfrak{m})^{-1}} \mathfrak{B}_{N-1}^{(\mathfrak{m})}. \tag{3.1b}$$

With this

$$\det \mathfrak{C}^{(\mathfrak{m})} = \prod_{i=1}^N \det \mathfrak{A}_i^{(\mathfrak{m})} \det \left\{ \mathrm{I} - (-1)^N \mathfrak{A}_N^{(\mathfrak{m})^{-1}} \mathfrak{B}_N^{(\mathfrak{m})} \mathfrak{A}_1^{(\mathfrak{m})^{-1}} \mathfrak{B}_1^{(\mathfrak{m})} \times \ldots \times \mathfrak{A}_{N-1}^{(\mathfrak{m})^{-1}} \mathfrak{B}_{N-1}^{(\mathfrak{m})} \right\} =$$

$$\prod_{i=1}^N \det \mathfrak{A}_i^{(\mathfrak{m})} \det \left(\mathfrak{A}_N^{(\mathfrak{m})^{-1}} \mathfrak{B}_N^{(\mathfrak{m})} \right) \det \left\{ \mathfrak{B}_N^{(\mathfrak{m})^{-1}} \mathfrak{A}_N^{(\mathfrak{m})} - (-1)^N \mathfrak{A}_1^{(\mathfrak{m})^{-1}} \mathfrak{B}_1^{(\mathfrak{m})} \times \ldots \times \mathfrak{A}_{N-1}^{(\mathfrak{m})^{-1}} \mathfrak{B}_{N-1}^{(\mathfrak{m})} \right\} =$$

$$\prod_{i=1}^N \det \mathfrak{A}_i^{(\mathfrak{m})} \det \left\{ \mathrm{I} - (-1)^N \mathfrak{A}_1^{(\mathfrak{m})^{-1}} \mathfrak{B}_1^{(\mathfrak{m})} \times \ldots \times \mathfrak{A}_N^{(\mathfrak{m})^{-1}} \mathfrak{B}_N^{(\mathfrak{m})} \right\}. \tag{3.2}$$

To arrive at the last equality the term $\det \left(\mathfrak{A}_N^{(\mathfrak{m})^{-1}} \mathfrak{B}_N^{(\mathfrak{m})} \right)$ was moved to the end and merged with the matrix in the curly braces, relying on the fact that for the purpose of calculating the determinant a product of matrices might be reordered arbitrarily even for matrices that do not commute under multiplication. Calculation (3.2) implies two important conclusions. One, barring the possible singularity of any of the $\mathfrak{A}_i^{(\mathfrak{m})}$ matrices, the matrix in the curly braces is expected to be responsible for the practical exploration of the singular manifold. Two, the ability to perform the cyclic shifting executed in (3.2) permits to renumber the contiguity curves θ_i at will for the determinant calculation alone without doing so elsewhere.

The compatibility manifold is defined by condition (2.4). For any number of sectors N this relation defines possible combinations of diffusivities and contiguity angles, for which a valid anisotropic solution exists. In axisymmetric geometries such as polar and spherical coordinates this manifold was degenerate in the sense that the solution was not encumbered by such a condition. Broken axial symmetry notwithstanding, the number of permissible layouts $\{\theta_i\}_{i=1}^N$ and diffusivities $\{K_i\}_{i=1}^N$ is still infinite.

(a) Two sectors

The two sector configurations are the simplest, yet useful in the analysis of more complicated layouts. The compatibility condition (2.4) reduces to $\cos(2\theta_2) - \cos(2\theta_1) = 0$, defining four relations $\theta_{i+1}(\theta_i)$, $i = 1$, for which anisotropic solutions exist:

$$\begin{array}{lll} \text{(a)} & \theta_{i+1} = \theta_i + \pi, & 0 \leqslant \theta_i < \pi \\ \text{(b)} & \theta_{i+1} = \pi - \theta_i, & 0 \leqslant \theta_i < \pi/2 \\ \text{(c)} & \theta_{i+1} = 2\pi - \theta_i, & 0 \leqslant \theta_i < \pi \\ \text{(d)} & \theta_{i+1} = 3\pi - \theta_i, & \pi \leqslant \theta_i < 3\pi/2. \end{array} \tag{3.3}$$

As is shown hereunder, relations (3.3) pertain to configurations of a higher number of sectors as well. For this reason the subscript notation of two generic adjacent sectors was retained. For easier visualisation these layouts are depicted in figure 3. Note that group (c) unifies two sub-groups labelled as (c_1) and (c_2). The determinant of $\mathfrak{C}^{(m)}$ vanishes when

$$\cos\bigl(2m(\theta_2 - \theta_1)\bigr) = 1. \tag{3.4}$$

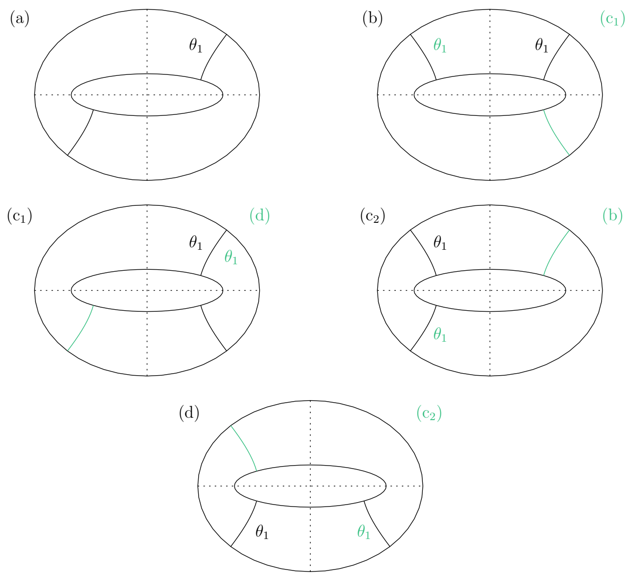

Figure 3: Partially symmetric compatible configurations for two sectors (black contiguity curves only; black labels conform to (3.3) with $i = 1$) and three sectors (all contiguity curves; green / grey labels conform to (3.3) with $i = 2$).

System (2.5) with $m = 2$ is insoluble only if $\theta_2 - \theta_1 = \pi/2, 3\pi/2$, i.e. an anisotropic solution exists for all four foregoing cases. Basic harmonics with $m \neq 2$ appear when (3.4) is satisfied. For instance, $m = 1$ gives $\theta_2 - \theta_1 = \pi$, i.e. group (a) in (3.3) includes the degrees of freedom associated with $m = 1$ in its entirety. Any basic harmonic $m \geqslant 3$ implies $\theta_2 - \theta_1 = \pi\ell/m$, where ℓ is an integer satisfying $1 \leqslant \ell \leqslant m - 1$. Thus any pair ℓ, m corresponds to a unique configuration in each of the groups (b) – (d) in (3.3):

$$\begin{array}{llllll} \text{(b)} & \theta_1 = \pi(1 - \ell/m)/2 & \text{(c)} & \theta_1 = \pi(2 - \ell/m)/2 & \text{(d)} & \theta_1 = \pi(3 - \ell/m)/2 \\ & \theta_2 = \pi(1 + \ell/m)/2 & & \theta_2 = \pi(2 + \ell/m)/2 & & \theta_2 = \pi(3 + \ell/m)/2. \end{array} \tag{3.5}$$

For proofs and additional technical detail regarding singular manifolds defined by $\det \mathfrak{C}^{(m)}$ the reader is referred to [12].

By contrast, elliptic harmonics are not encumbered by a restriction on any specific value of $\mathfrak{m}$. Thus any configuration in (3.3), for which $\det \mathfrak{C}^{(\mathfrak{m})} = 0$, admits the associated degrees of freedom. Using the central line in (3.2) and swapping the indices 1 and 2 yields

$$\det \mathfrak{C}^{(\mathfrak{m})} = \det \mathfrak{A}_2^{(\mathfrak{m})} \det \mathfrak{B}_1^{(\mathfrak{m})} \det \left({\mathfrak{B}_1^{(\mathfrak{m})}}^{-1} \mathfrak{A}_1^{(\mathfrak{m})} - {\mathfrak{A}_2^{(\mathfrak{m})}}^{-1} \mathfrak{B}_2^{(\mathfrak{m})} \right) \tag{3.6a}$$

provided that $\mathfrak{B}_1^{(\mathfrak{m})}$ and $\mathfrak{A}_2^{(\mathfrak{m})}$ are invertible. Generally this is not a trivial conclusion: whilst $\det \mathfrak{B}_1^{(\mathfrak{m})} = k_1 W_{\mathfrak{m}}(\theta_1)$ and $\det \mathfrak{A}_2^{(\mathfrak{m})} = W_{\mathfrak{m}}(\theta_2)$ have a Wronskian-like pattern with

$$W_{\mathfrak{m}}(\theta_i) = \mathrm{se}_{\mathfrak{m}}(\theta_i)\,\mathrm{ce}'_{\mathfrak{m}}(\theta_i) - \mathrm{se}'_{\mathfrak{m}}(\theta_i)\,\mathrm{ce}_{\mathfrak{m}}(\theta_i),$$

the functions $\mathrm{se}_{\mathfrak{m}}$ and $\mathrm{ce}_{\mathfrak{m}}$ do not constitute a pair of independent solutions to (2.10b) with the same value of a. The Wronskian of (2.10b) is a constant function, but the Wronskian of the equation, whose two independent solutions are $\mathrm{se}_{\mathfrak{m}}$ and $\mathrm{ce}_{\mathfrak{m}}$, is not, and there is no elegant result as to its roots. Thus in theory it is possible that in some instances $W_{\mathfrak{m}}$ vanishes. In practice none of the extensive parametric scans run for a variety of $\mathfrak{m}$, q and θ values yielded such an example.

The calculation in (3.6a) for the four groups of configurations in (3.3) with the aid of trigonometric identities applied to (2.11a) is technical, but elementary:

$$\mathfrak{A}_i^{(\mathfrak{m})^{-1}}\mathfrak{B}_i^{(\mathfrak{m})} = \frac{1}{W_{\mathfrak{m}}}\begin{pmatrix} \mathrm{se}'_{\mathfrak{m}}\,\mathrm{ce}_{\mathfrak{m}} - k_i\,\mathrm{se}_{\mathfrak{m}}\,\mathrm{ce}'_{\mathfrak{m}} & (1-k_i)\,\mathrm{ce}_{\mathfrak{m}}\,\mathrm{ce}'_{\mathfrak{m}} \\ (k_i-1)\,\mathrm{se}_{\mathfrak{m}}\,\mathrm{se}'_{\mathfrak{m}} & k_i\,\mathrm{se}'_{\mathfrak{m}}\,\mathrm{ce}_{\mathfrak{m}} - \mathrm{se}_{\mathfrak{m}}\,\mathrm{ce}'_{\mathfrak{m}} \end{pmatrix}\Bigg|_{\theta_i}, \tag{3.6b}$$

whilst $\mathfrak{B}_i^{(\mathfrak{m})^{-1}}\mathfrak{A}_i^{(\mathfrak{m})} = \mathfrak{A}_i^{(\mathfrak{m})^{-1}}\mathfrak{B}_i^{(\mathfrak{m})}\Big|_{k_i \longmapsto 1/k_i}$. The identity $\mathrm{ce}_{\mathfrak{m}}(\theta_2) = (-1)^m\,\mathrm{ce}_{\mathfrak{m}}(\theta_1)$ holds for all groups in

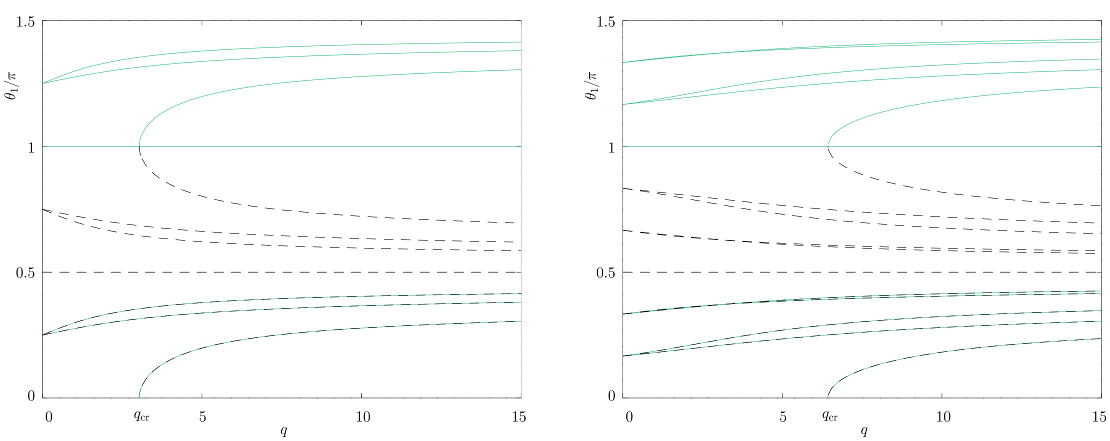

Figure 4: Compatible two sector configurations for elliptic harmonics $\mathfrak{m} = 2$ (left) and $\mathfrak{m} = 3$ (right). Curve colour and style correspond to (3.3) with $i = 1$: dashed green / grey (b), dashed black (c), solid green / grey (d).

(3.3), whilst for group (a) $\mathrm{se}_{\mathfrak{m}}(\theta_2) = (-1)^m\,\mathrm{se}_{\mathfrak{m}}(\theta_1)$, and $\mathrm{se}_{\mathfrak{m}}(\theta_2) = -(-1)^m\,\mathrm{se}_{\mathfrak{m}}(\theta_1)$ for (b)–(d). Thus for group (a) the matrix $\mathfrak{B}_1^{(\mathfrak{m})^{-1}}\mathfrak{A}_1^{(\mathfrak{m})} - \mathfrak{A}_2^{(\mathfrak{m})^{-1}}\mathfrak{B}_2^{(\mathfrak{m})}$ in (3.6a) is the zero matrix for any $\mathfrak{m}$ and θ_1, ergo when the ellipse is divided into two equal sectors (of any orientation), all elliptic harmonics are permissible in (2.12). For groups (b) – (d) the foregoing matrix has zero entries on the main diagonal, resulting in

$$\det \mathfrak{C}^{(\mathfrak{m})} = 4k_1(1-k_2)^2\,\mathrm{ce}_{\mathfrak{m}}(\theta_1)\,\mathrm{ce}'_{\mathfrak{m}}(\theta_1)\,\mathrm{se}_{\mathfrak{m}}(\theta_1)\,\mathrm{se}'_{\mathfrak{m}}(\theta_1). \tag{3.6c}$$

Thus $\det \mathfrak{C}^{(\mathfrak{m})}$ vanishes at the roots and critical points of the functions $\mathrm{ce}_{\mathfrak{m}}, \mathrm{se}_{\mathfrak{m}}$, independently of k_i and similarly to the basic harmonics in (3.4). Thus the only dependence of interest is that on q. Figure 4 depicts the variation of the roots of $\det \mathfrak{C}^{(\mathfrak{m})}$ with q for different values of $\mathfrak{m}$. The first observation is that $\theta = 0, \pi/2, \pi$

are always either a root or critical point of each the four functions in (2.11a), whereby the angles $\theta_1 = \pi/2, \pi$ form horizontal symmetry lines for $\theta_1(q)$. The remaining roots of $\det \mathfrak{C}^{(\mathfrak{m})}$ can only be computed numerically. For sufficiently small q they come in pairs, whose number increases with $\mathfrak{m}$. The shape resembles a blade of grass with the tip at $q = 0$, where the pair of roots merges. There exists a critical value q_{cr}, above which either one (groups (b) and (d) in (3.3)) or two (group (c) in (3.3)) new unpaired branches appear. The abscissa variable q is directly related to the eigenvalues endowed by the Sturm-Liouville problem of (2.10c) with appropriate boundary conditions. The salient conclusion following from the qualitative form of $\theta_1(q; \mathfrak{m})$ is twofold: for any value of q there are multiple values of θ_1, implying that regardless of the interval and boundary conditions in (2.10c) a number of viable anisotropic configurations exists; this number grows with the elliptic harmonic frequency $\mathfrak{m}$, but is constant for each $\mathfrak{m}$ below and above q_{cr}. The symmetric layouts with $\theta_1 = 0,\ \pi/2$ allow elliptic harmonics of any $\mathfrak{m}$ and q, i.e. any boundary conditions for (2.10c) that result in a soluble Sturm-Liouville problem. Some configurations support combinations of an elliptic harmonic $\mathfrak{m}$ and a basic harmonic m, obtained by locating intersections of the curves in figure 4 with the horizontal lines θ_1 in (3.5).

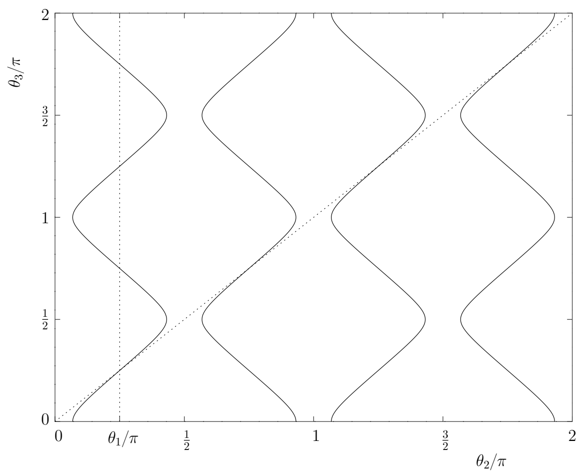

Figure 5: Manifold (3.7) with $K_1 = 1$, $K_2 = 10$, $K_3 = 0.1$ and $\theta_1 = \frac{\pi}{4}$. Dotted lines mark the subdomain $\theta_1 < \theta_2 < \theta_3$.

(b) Three sectors

The compatibility condition (2.4) for a 3-sector configuration might be re-written as

$$\left(\frac{1}{K_1} - \frac{1}{K_2}\right)\cos(2\theta_1) + \left(\frac{1}{K_2} - \frac{1}{K_3}\right)\cos(2\theta_2) + \left(\frac{1}{K_3} - \frac{1}{K_1}\right)\cos(2\theta_3) = 0. \tag{3.7}$$

Figure 5 shows a typical example of the manifold shape for $N = 3$. Out of the four strands that stem from the double frequencies present in (2.4) only configurations satisfying $\theta_1 < \theta_2 < \theta_3$ are valid. The diffusivities K_i affect the amplitude of $\theta_2(\theta_3)$ or equivalently the horizontal distance between the strands. Depending on the relative magnitude of the factors preceding the cosines in (3.7), the strands might be oriented horizontally instead. To pinpoint layouts that accord elliptic harmonics, one must traverse the permissible portion of each strand and calculate $\det \mathfrak{C}^{(\mathfrak{m})}$. As the number of sectors grows, accurate numerical identification of layouts, where $\det \mathfrak{C}^{(\mathfrak{m})} = 0$, becomes increasingly difficult since $\mathfrak{C}^{(\mathfrak{m})}$ are ill-conditioned near the sought singularities. Thus locating symmetries that lead to analytical insight is even more important than for two sectors.

An immediate observation is that if $\cos(2\theta_i) = \cos(2\theta_{i+1})$ for any two adjacent angles, then all three $\cos(2\theta_i)$ in (3.7) must equal. This defines a family of symmetric compatible configurations related to (3.3): since groups (b)–(d) are mutually exclusive, the only way to ensure that (3.3) are satisfied pairwise for every two angles out of three, is to add a contiguity curve from (a) to any layout in groups (b)–(d). Figure 3 depicts this construction and associated renumbering. For the purpose of calculating $\det \mathfrak{C}^{(\mathfrak{m})}$ renumber θ_i so that θ_1 and θ_2 satisfy (a), and the remaining contiguity curve is θ_3. Then for any two adjacent angles by (3.6b)

$$\mathfrak{A}_i^{(\mathfrak{m})^{-1}}\mathfrak{B}_i^{(\mathfrak{m})}\mathfrak{A}_{i+1}^{(\mathfrak{m})^{-1}}\mathfrak{B}_{i+1}^{(\mathfrak{m})} = \frac{1}{W_\mathfrak{m}}\begin{pmatrix} k_i k_{i+1}\operatorname{se}_\mathfrak{m}\operatorname{ce}'_\mathfrak{m} - \operatorname{se}'_\mathfrak{m}\operatorname{ce}_\mathfrak{m} & (k_i k_{i+1}-1)\operatorname{ce}_\mathfrak{m}\operatorname{ce}'_\mathfrak{m} \\ (1-k_i k_{i+1})\operatorname{se}_\mathfrak{m}\operatorname{se}'_\mathfrak{m} & \operatorname{se}_\mathfrak{m}\operatorname{ce}'_\mathfrak{m} - k_i k_{i+1}\operatorname{se}'_\mathfrak{m}\operatorname{ce}_\mathfrak{m}\end{pmatrix}\Bigg|_{\theta_i}. \tag{3.8}$$

Then using the form given in the middle line of (3.2) with $N = 3$ and the reversed product below (3.6b) with $1/k_3 = k_1 k_2$ yields

$$\det \mathfrak{C}^{(m)} = 4k_3(1-k_1k_2)^2 W_\mathfrak{m}(\theta_1)\operatorname{ce}_\mathfrak{m}(\theta_1)\operatorname{ce}'_\mathfrak{m}(\theta_1)\operatorname{se}_\mathfrak{m}(\theta_1)\operatorname{se}'_\mathfrak{m}(\theta_1). \tag{3.9}$$

A comparison between (3.9) and (3.6c) makes it obvious that, bar any roots of $W_\mathfrak{m}(\theta_1)$, figure 4 suffices to provide the dependence of the $\mathfrak{m}$-harmonic admitting layout $\{\theta_i\}$ on q with the ordinate θ_1 as marked in figure 3.

(c) Four and more sectors

Cyclic shifting of (3.2) for $N = 4$ allows to infer that

$$\begin{aligned}\det \mathfrak{C}^{(\mathfrak{m})} = \det(\mathfrak{A}_1^{(\mathfrak{m})})\det(\mathfrak{A}_2^{(\mathfrak{m})})\det(\mathfrak{B}_3^{(\mathfrak{m})})\det(\mathfrak{B}_4^{(\mathfrak{m})})\times \\ \det\left(\mathfrak{B}_4^{(\mathfrak{m})^{-1}}\mathfrak{A}_4^{(\mathfrak{m})}\mathfrak{B}_3^{(\mathfrak{m})^{-1}}\mathfrak{A}_3^{(\mathfrak{m})} - \mathfrak{A}_1^{(\mathfrak{m})^{-1}}\mathfrak{B}_1^{(\mathfrak{m})}\mathfrak{A}_2^{(\mathfrak{m})^{-1}}\mathfrak{B}_2^{(\mathfrak{m})}\right).\end{aligned} \tag{3.10}$$

A result similar to (3.9) follows when the angles θ_i are related to one another as in figure 3, i.e. form a configuration that is symmetric under reflexion across both the horizontal and vertical axes: for some $0 < \theta_1 < \pi/2$, the rest of the angles are $\theta_2 = \pi - \theta_1$, $\theta_3 = \pi + \theta_1$ and $\theta_4 = 2\pi - \theta_1$. The matrix $\mathfrak{A}_1^{(\mathfrak{m})^{-1}}\mathfrak{B}_1^{(\mathfrak{m})}\mathfrak{A}_2^{(\mathfrak{m})^{-1}}\mathfrak{B}_2^{(\mathfrak{m})}$ follows immediately by (3.8). The matrix $\mathfrak{B}_4^{(\mathfrak{m})^{-1}}\mathfrak{A}_4^{(\mathfrak{m})}\mathfrak{B}_3^{(\mathfrak{m})^{-1}}\mathfrak{A}_3^{(\mathfrak{m})}$ might be obtained via (3.8) by mapping

$$\mathfrak{B}_{i+1}^{(\mathfrak{m})^{-1}}\mathfrak{A}_{i+1}^{(\mathfrak{m})}\mathfrak{B}_i^{(\mathfrak{m})^{-1}}\mathfrak{A}_i^{(\mathfrak{m})} = \mathfrak{A}_{i+1}^{(\mathfrak{m})^{-1}}\mathfrak{B}_{i+1}^{(\mathfrak{m})}\Big|_{k_{i+1}\longmapsto 1/k_{i+1}}\mathfrak{A}_i^{(\mathfrak{m})^{-1}}\mathfrak{B}_i^{(\mathfrak{m})}\Big|_{k_i\longmapsto 1/k_i}.$$

With $1/(k_3k_4) = k_1k_2$

$$\det \mathfrak{C}^{(m)} = 4k_3k_4(1-k_1k_2)^2 W_\mathfrak{m}^2(\theta_1)\operatorname{ce}_\mathfrak{m}(\theta_1)\operatorname{ce}'_\mathfrak{m}(\theta_1)\operatorname{se}_\mathfrak{m}(\theta_1)\operatorname{se}'_\mathfrak{m}(\theta_1), \tag{3.11}$$

again leading to the conclusion that the compatibility of symmetric four sector configurations for elliptic harmonics is fully described by figure 4. $N = 4$ is the largest number of partitions that is fully amenable to considerations of reflexion symmetry.

The theory for symmetric layouts developed above might be extended via mathematical induction for a higher number of subdomains. The following lemma allows to reduce a layout of N subdomains to one of $N-1$, provided that any two (not necessarily adjacent) contiguity curves satisfy $\cos(2\theta_i) = \cos(2\theta_j)$ for $i \neq j$.

Lemma 3.1 *Let a configuration defined by layout* $\{\theta_i\}_{i=1}^N$ *and respective set of diffusivities* K_i *satisfy the compatibility condition (2.4) with* $\cos(2\theta_i) = \cos(2\theta_j)$ *for some* $1 \leqslant i < j < N$. *Then if*

$$\frac{1}{K_i} + \frac{1}{K_j} \neq \frac{1}{K_{i+1}} + \frac{1}{K_{j+1}}, \tag{3.12a}$$

the reduced configuration of $N-1$ *sectors* $\{\vartheta_\ell\}$ *with respective* $\{\mathcal{K}_\ell\}$ *such that*

$$\vartheta_\ell = \theta_\ell, \quad \frac{1}{\mathcal{K}_\ell} = \begin{cases} \dfrac{1}{K_\ell} + \dfrac{1}{K_{i+1}} & \ell = 1, \ldots, i-1, j+1, \ldots, N \\[2ex] \dfrac{1}{K_\ell} + \dfrac{1}{K_i} & \ell = i+1, \ldots, j \end{cases} \tag{3.12b}$$

also satisfies (2.4). If condition (3.12a) does not hold, the reduced configuration of $N-2$ *sectors* $\{\vartheta_\ell\}$ *with respective* $\{\mathcal{K}_\ell\}$ *such that*

$$\vartheta_\ell = \theta_\ell, \quad \frac{1}{\mathcal{K}_\ell} = \begin{cases} \dfrac{1}{K_\ell} + \dfrac{1}{K_{i+1}} & \ell = 1, \ldots, i-1, j+1, \ldots, N \\[2ex] \dfrac{1}{K_\ell} + \dfrac{1}{K_i} & \ell = i+1, \ldots, j-1 \end{cases} \tag{3.12c}$$

also satisfies (2.4).

Proof Write out the compatibility condition (2.4) as

$$\left(\frac{1}{K_1} - \frac{1}{K_2}\right)\cos(2\theta_1) + \ldots + \left(\frac{1}{K_i} - \frac{1}{K_{i+1}}\right)\cos(2\theta_i) + \ldots +$$
$$\left(\frac{1}{K_j} - \frac{1}{K_{j+1}}\right)\cos(2\theta_j) + \ldots + \left(\frac{1}{K_N} - \frac{1}{K_1}\right)\cos(2\theta_N) = 0. \tag{3.13}$$

Define $\vartheta_\ell = \theta_\ell$ for all $1 \leqslant \ell \leqslant i-1$ and $i+1 \leqslant \ell \leqslant N$, i.e. the partition of the reduced configuration simply skips θ_i. In order for it to satisfy (2.4), the reciprocals of the new diffusivities $\mathcal{K}_i$ must satisfy the following linear system of size $N-1$:

$$\begin{pmatrix} 1 & -1 & & & \\ & 1 & -1 & & \\ & & \ddots & \ddots & \\ & & & 1 & -1 \\ -1 & & & & 1 \end{pmatrix} \begin{pmatrix} 1/\mathcal{K}_1 \\ \vdots \\ 1/\mathcal{K}_{i-1} \\ 1/\mathcal{K}_{i+1} \\ \vdots \\ 1/\mathcal{K}_N \end{pmatrix} = \begin{pmatrix} 1/K_1 - 1/K_2 \\ \vdots \\ 1/K_{i-1} - 1/K_i \\ 1/K_{i+1} - 1/K_{i+2} \\ \vdots \\ 1/K_{j-1} - 1/K_j \\ 1/K_j - 1/K_{j+1} + 1/K_i - 1/K_{i+1} \\ 1/K_{j+1} - 1/K_{j+2} \\ \vdots \\ 1/K_N - 1/K_1 \end{pmatrix}. \tag{3.14}$$

The right-hand side entry at row $j-1$ follows from $\cos(2\theta_i) = \cos(2\theta_j)$.

System (3.14) is singular: the sum of all rows of the matrix results in the zero vector. Since the first $N-2$ rows are independent, the rank of this matrix is $N-2$. For a non-trivial solution to exist the right-hand side vector must lie in the kernel of the transposed matrix. In this case the rank deficiency is 1 and the linear combination of matrix rows giving the zero vector is a simple sum, whereby if the sum of entries of the right-hand side vector equals zero, a non-trivial solution with exactly one degree of freedom must exist. The verification that the right-hand side vector sums to zero is immediate.

To conclude the proof one must construct a sequence $\{\mathcal{K}_\ell\}$, $\ell = \{1, \ldots, i-1, i+1, \ldots, N\}$, whose entries are positive with no two adjacent values matching. Although this sequence might not be unique, one such construction suffices. Keeping $\mathcal{K}_1$ as a degree of freedom, (3.14) yields

$$\frac{1}{\mathcal{K}_\ell} = \begin{cases} \dfrac{1}{\mathcal{K}_1} - \dfrac{1}{K_1} + \dfrac{1}{K_\ell} & \ell = 2, \ldots, i-1, j+1, \ldots, N \\[2ex] \dfrac{1}{\mathcal{K}_1} - \dfrac{1}{K_1} + \dfrac{1}{K_i} & \ell = i+1 \\[2ex] \dfrac{1}{\mathcal{K}_1} - \dfrac{1}{K_1} + \dfrac{1}{K_i} - \dfrac{1}{K_{i+1}} + \dfrac{1}{K_\ell} & \ell = i+2, \ldots, j. \end{cases} \tag{3.15a}$$

By observation no two adjacent entries $\mathcal{K}_\ell$ coincide by virtue of similarly distinct K_ℓ except for $\ell = j$ and $\ell = j+1$. To have $\mathcal{K}_j \neq \mathcal{K}_{j+1}$ condition (3.12a) must hold. At this point set

$$\frac{1}{\mathcal{K}_1} = \frac{1}{K_1} + \frac{1}{K_{i+1}}, \tag{3.15b}$$

rendering all $\mathcal{K}_\ell > 0$ and giving (3.12b). If (3.12a) does not hold, the terms with $\cos(2\theta_i)$ and $\cos(2\theta_j)$ in (3.13) cancel. Number the remaining sectors from 1 to N, skipping both i and j. A process identical to the above gives a system of $N-2$ equations, with only $N-3$ independent, resulting in (3.12c). The only non-trivial check is that $\mathcal{K}_{j-1} \neq \mathcal{K}_{j+1}$. Using (3.12c) and (3.12a) reduces this negation to $K_j \neq K_{j+1}$, which holds by the assumption on the original set $\{K_\ell\}$. ■

4 Critical points of mixed type

The presence of anisotropy allows for a critical point that combines saddle-node characteristics. The necessary condition for such a point to come into existence is to be located on the contiguity surface θ_i between two sectors. Condition (1.5b) means that on two sides of any θ_i the derivative u_θ is discontinuous except when it vanishes. Consider a regular Sturm-Liouville problem over an elliptic cylinder with (2.10c) satisfying $Z_n'(0) = Z_n'(1) = 0$. On an elliptic cylinder shell of a fixed value of ξ the contiguity curves are straight lines and the solution is symmetric about $\zeta = \frac{1}{2}$. Taking all input parameters as in figure 2, using just one 3D component in (2.12) corresponding to $n = 2$ and tuning $\alpha_{2,2}^{(1)}$ results in the isocontour map in figure 6. Six of the critical points on the symmetry line $\zeta = \frac{1}{2}$ are regular: four nodes and 2 saddles (black diamonds), whilst two are of the mixed type (green / grey diamonds): the curvature of the contours on one side of the contiguity border θ_i is characteristic of a saddle, but on the other side the behaviour is node-like. The creation of this unconventional type of critical point might be viewed as a collision of one saddle and one node moving toward the contiguity line from two sides when the parameters are tuned. It must be noted that nodes seen in cross-sectional contour maps as in figure 6 are not local minima or maxima, since the maximum principle prevents such an occurrence.

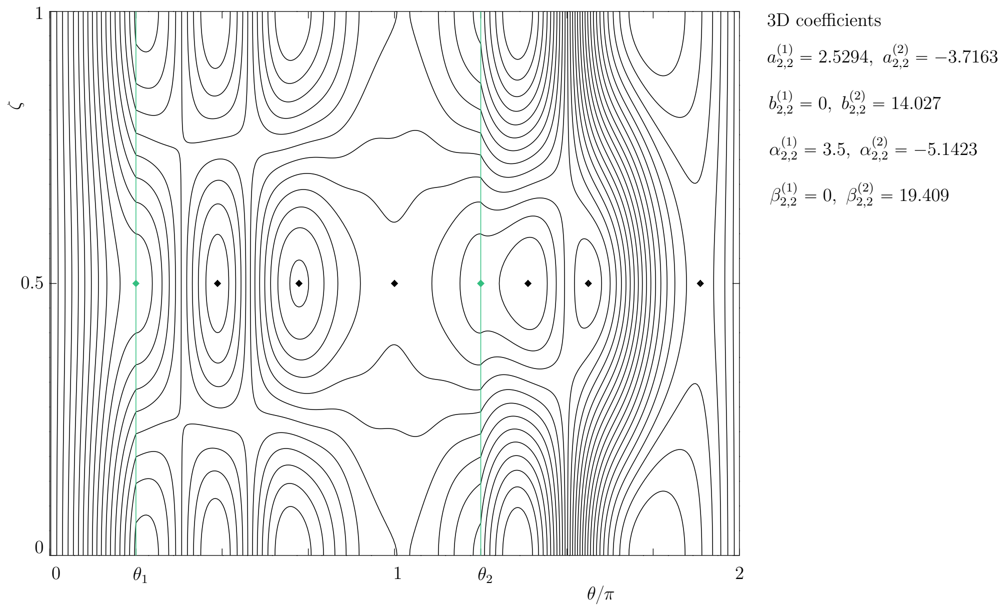

Figure 6: Isocontour map of (2.12) with $m = 2$ and $m = 12$ over the (θ, ζ) plane at the elliptic shell $\xi = (\xi_{\text{in}} + \xi_{\text{ex}})/2$ for the Sturm-Liouville problem $Z'(0) = Z'(1) = 0$; all parameters and 2D coefficients as in figure 2; coefficient values as stated (given to 5 significant figures); contour level linearly distributed (density corresponds to gradient). Black diamonds: regular critical points, green / grey diamonds: mixed type critical points.

5 Positivity

The positivity of solutions to (1.1) is a desired property similarly to related elliptic or parabolic equations. Most of the reasoning below holds for any system of coordinates, where an anisotropic solution to (1.1) exists. Infra θ denotes the coordinate that traces closed orbits in Cartesian space and together with ξ forms the plane, where the periodic anisotropy partition is defined, and ζ is normal thereto. Define Ω_i as the support domain of solution u_i:

$$\Omega_i = \Big\{(\xi, \theta, \zeta) \;\Big|\; \xi_{\text{in}} \leqslant \xi \leqslant \xi_{\text{out}},\, \theta_{i-1} \leqslant \theta \leqslant \theta_i,\, \zeta \in I, \Big\}, \quad 1 \leqslant i \leqslant N,$$

where the index i outside of the indicated range is wrapped as required by periodicity, and the interval I might be finite or infinite as in corollary 2.1, or redundant for a planar setting. The full domain is $\Omega = \bigcup_{i=1}^{N} \Omega_i$, and the contiguity surface between Ω_i and Ω_{i+1} is Γ_i. Equation (1.1) is linear in $\tilde{u} = u^\gamma$ and henceforth the discussion focusses on $\tilde{u}$, since its positivity guarantees the positivity of u. The function $\tilde{u}_i$ is the restriction of $\tilde{u}$ to Ω_i. It is possible to divide $\tilde{u}_i$ into two components $\tilde{u}_i = \tilde{u}_{i,\text{h}} + \tilde{u}_{i,\text{sh}}$, where $\tilde{u}_{i,\text{h}}$ is harmonic ($\Delta\tilde{u}_{i,\text{h}} = 0$) and $\tilde{u}_{i,\text{sh}}$ is strictly subharmonic ($\Delta\tilde{u}_{i,\text{sh}} > 0$) or superharmonic ($\Delta\tilde{u}_{i,\text{sh}} < 0$) [15, ch. 2, §1] for any $C \neq 0$, as well as free of any harmonic components. Since the equation is linear, this requirement is fulfilled by verifying none of the summands satisfy its homogeneous part. In (2.1) and (2.9) such division corresponds to the homogeneous and inhomogeneous parts. The function $\tilde{u}_{i,\text{h}}$ is in $C^2(\Omega_i) \cap C(\partial\Omega_i)$, but it is also 2π-periodic and thus in $C^2(\Omega) \cap C(\partial\Omega)$, and harmonic not only in Ω_i, but in Ω. The extension to Ω is denoted by $\tilde{u}_{i,\mathrm{h}}\big|_{\Omega}$ and is not to be confused with $\tilde{u}$, which is neither harmonic nor in the above continuity class (it is infinitely differentiable with respect to ξ and ζ, but the derivative $\partial_\theta \tilde{u}$ is discontinuous on all Γ_i).

The sufficient conditions for the positivity of $\tilde{u}$ rely on the maximum principle for elliptic operators. As aspects from its proof are required for inferences in the anisotropic setting, it is briefly restated following [16].[1] Suppose $f \in C^2(\Omega) \cap C(\partial\Omega)$ and $\nabla \cdot (K\nabla f) \geqslant 0$ with $K > 0$. Define $w = \max\limits_{\Omega}\Big\{f - \max\limits_{\partial\Omega} f, 0\Big\}$. Observe that $w \geqslant 0$ since $\min\limits_{\Omega} w = 0$. Locate the largest set $\Omega_o \subset \Omega$ such that $w = f - \max\limits_{\partial\Omega} f > 0$ in $\Omega_o \backslash \partial\Omega_o$ and $w = 0$ on $\partial\Omega_o$. Then if Ω_o is not empty,

$$0 \leqslant \int\limits_{\Omega_o} w\nabla \cdot (K\nabla f)\mathrm{d}V = -\int\limits_{\Omega_o} (\nabla w) \cdot (K\nabla f)\mathrm{d}V = -\int\limits_{\Omega_o} K\big|\nabla w\big|^2 \mathrm{d}V \leqslant 0, \tag{5.1a}$$

where a corollary of the divergence theorem (Green's identity) was used:

$$\int\limits_{\Omega_o} \nabla \cdot (wK\nabla f)\mathrm{d}V = \int\limits_{\Omega_o} \Big\{w\nabla \cdot (K\nabla f) + (\nabla w) \cdot (K\nabla f)\Big\}\mathrm{d}V = \oint\limits_{\partial\Omega_o} \Big(wK\nabla f \cdot \hat{n}\Big)\mathrm{d}S = 0, \tag{5.1b}$$

with the integrals denoting volume or area and surface or contour integration depending on the dimension of Ω_o. The inequalities in (5.1a) are only possible if $w \equiv 0$ in Ω and thus $\max\limits_{\Omega} f = \max\limits_{\partial\Omega} f$. Similarly suppose $\nabla \cdot (K\nabla f) \leqslant 0$ and define $w = \min\limits_{\Omega}\Big\{f - \min\limits_{\partial\Omega} f, 0\Big\}$. Now $w \leqslant 0$ and (5.1a) still holds, yielding $\min\limits_{\Omega} f = \min\limits_{\partial\Omega} f$. Both inferences hold if $\nabla \cdot (K\nabla f) = 0$, whence $\min\limits_{\partial\Omega} f \leqslant f \leqslant \max\limits_{\partial\Omega} f$.

It therefore follows that positive boundary conditions on $\partial\Omega$ for the extended function $\tilde{u}_{i,\mathrm{h}}\big|_{\Omega}$ suffice to have $\tilde{u}_{i,\mathrm{h}} > 0$ in Ω_i. However, the infimum and supremum of $\tilde{u}_{i,\mathrm{h}}$ might be tighter than those provided by $\tilde{u}_{i,\mathrm{h}}\big|_{\Omega}$. In fact, it is possible to have $\tilde{u}_{i,\mathrm{h}} > 0$ without $\tilde{u}_{i,\mathrm{h}}\big|_{\Omega} > 0$. Furthermore, the bounds of $\tilde{u}_{i,\mathrm{h}}$ fall on the boundary $\partial\Omega_i$, which includes the surfaces Γ_{i-1} and Γ_i that except for $\partial\Gamma_{i-1}, \partial\Gamma_i$ are in the interior of Ω. The harmonic part of $\tilde{u}$, denoted by $\tilde{u}_{\mathrm{h}}$, is the collection of restrictions $\tilde{u}_{i,\mathrm{h}}$. To have $\tilde{u}_{\mathrm{h}} > 0$ in Ω, a simple, but overly restrictive sufficient condition is $\tilde{u}_{i,\mathrm{h}}\big|_{\Omega} > 0$ on $\partial\Omega$ for all i. A necessary and sufficient, but harder to implement condition is $\tilde{u}_{i,\mathrm{h}} > 0$ on $\partial\Omega_i$ for all i. The conceptual distinction between a boundary condition in a classical setting and the anisotropic problem here is that the condition is only prescribed on $\partial\Omega_{i_*} \backslash (\Gamma_{i_*-1} \cup \Gamma_{i_*})$ for one index i_*. Thus the anisotropic solution might attain a minimum or maximum at an interior point in Ω on any Γ_i when $C = 0$, but it might not be a classical node, even if all three components of $\nabla\tilde{u}$ vanish thereat, because the behaviour on each side of Γ_i is determined by the distinct functions $\tilde{u}_{i,\mathrm{h}}$ and $\tilde{u}_{i+1,\mathrm{h}}$.

To complete the argument one must look at $\tilde{u}_{\mathrm{sh}}$, the collection of $\tilde{u}_{i,\mathrm{sh}}$. From (1.1)

$$\nabla \cdot \big(K\nabla\tilde{u}\big) = -\gamma C. \tag{5.2}$$

Define an auxiliary problem $\Delta\tilde{u}_+ = 1$, where the sought function $\tilde{u}_+$ is free of harmonic components. In polar and spherical coordinates $\tilde{u}_+ = \xi^2/2$ and $\tilde{u}_+ = \xi^2/6$ respectively. In the elliptic coordinates $\tilde{u}_+ = f^2\Big(\cosh(2\xi) + \cos(2\theta)\Big)\Big/8$. In all three cases $\tilde{u}_+ \geqslant 0$ and $\tilde{u}_+ = 0$ is only possible when $\xi = 0$. In the former two cases $\xi = 0$ is a point. In the elliptic coordinates it is a line joining the two foci, formally an ellipse of area zero. Moreover, $\partial_\xi\tilde{u}_+ \geqslant 0$, and again $\partial_\xi\tilde{u}_+ = 0$ only at $\xi = 0$. Since $\tilde{u}_+$ is subharmonic, it is bounded from above by a maximum attained on the boundary of the domain. If $\xi = 0$ is excluded from the domain, $\partial_\xi\tilde{u}_+ > 0$ implies that out of the two arcs of $\partial\Omega$ or $\partial\Omega_i$ corresponding to constant ξ, the maximum is attained on ξ_{out}.

[1] In [16] the term *anisotropic* refers to an unrelated framework, where the diffusivity tensor contains off-diagonal entries.

The solution to (5.2) in Ω_i is $\tilde{u}_{i,\mathrm{sh}} = -\gamma C \tilde{u}_+\big|_{\Omega_i}/K_i$. When $\gamma C < 0$, clearly $\tilde{u}_{i,\mathrm{sh}} > 0$, giving $\tilde{u}_i > 0$ in Ω_i and thence $\tilde{u} > 0$ in Ω. The "slack" $\min \tilde{u}_{\mathrm{sh}}$ might be used to lower the minimum of $\tilde{u}_{\mathrm{h}}$ to zero by simple addition. When $\gamma C > 0$, there are three options that ensure positivity of the sum $\tilde{u}_i = \tilde{u}_{i,\mathrm{h}} + \tilde{u}_{i,\mathrm{sh}}$. One, since a superharmonic function is bounded from below by a minimum on the boundary, it is possible to demand that the extensions $\tilde{u}_i\big|_{\Omega} > 0$ on $\partial\Omega$, or more restrictively $\tilde{u}_i > 0$ on $\partial\Omega_i$, for all i. Two, the monotonicity in ξ established above allows to infer that given a solution $\tilde{u}_{\mathrm{h}} > 0$, there exists $\xi_{\mathrm{out}} > 0$ small enough to ensure $\tilde{u} > 0$. Three, if the range of ξ is fixed, there exists C such that $|\gamma C|$ is small enough to achieve a similar outcome.

6 Conclusion

The successful construction of anisotropic solutions in elliptic cylinder coordinates shows that the axial symmetry inherent to cylindrical and spherical geometries is not essential. However, in the elliptic coordinate system a new compatibility condition is introduced as part of theorem 2.1, relating the anisotropic layout's contiguity angles and subdomain diffusivities. Whether the emergence of this condition is a direct result of the non-axisymmetric geometry or merely a peculiarity of this specific coordinate system, remains to be seen. A complete analysis of the remaining nine coordinate systems, where Laplace's equation is separable, will be able to determine that, but is outside of the ambit of this study. Compared to the unencumbered by such a compatibility condition cylindrical and polar coordinate systems, the set of all layouts, for which azimuthally anisotropic solutions exist, is somewhat limited, albeit still infinite. In the case of diffusion with no bulk source or sink, i.e. $C = 0$, no compatibility condition is needed.

Configurations with a high number of subdomains, but harbouring a partial symmetry $\cos(2\theta_i) = \cos(2\theta_j)$, $i \neq j$, might be reduced to an equivalent layout with fewer sectors. In practice the reduction is more effectively used in reverse: based on a configuration satisfying the compatibility condition (2.4), one constructs a family of configurations with one sector more, all of which still satisfy (2.4).

The number of harmonics incorporated into the solution is determined by the desired boundary conditions. Standard conditions (Dirichlet, Neumann or Robin) might be imposed on the boundaries of any one sector, identically to the isotropic setting. The conditions on the complement boundary follow by continuity of u and its azimuthal flux, resulting in linear systems for the coefficients in both 2D and 3D solutions. For a degree of freedom to be available for use in boundary conditions, the associated homogeneous linear system must be singular. The only exception is the $m = 2$ harmonic in the 2D part of the solution, for which the linear system is inhomogeneous when $C \neq 0$, and thus must be non-singular. The variety and complexity of topological features accorded by even a few harmonics is remarkable, i.e. the inclusion of any degrees of freedom responsible for tangential velocity components (the equivalent of azimuthal velocity in an axisymmetric geometry) induces strong gradients and thus momentum transfer in both ξ and θ directions. The presence of numerous critical points means the diffusing particles are likely to spend prolonged periods of time trapped in regions with low velocities.

When an isolated critical point is situated on the contiguity curve between two subdomains of distinct diffusivities, it is possible that the point's type, as determined by the topological terrain on two sides of the curve, is mismatched: node on one side and saddle on the other. One of the consequences of such an occurrence is that although the half-node might be stable, its pairing with a half-saddle renders the critical point unstable overall. Furthermore, the saddle-node pairings create a conceptual gradation that bridges the extremes of stable and unstable nodes. Figure 7 illustrates this effect. For simplicity consider a surface oriented in space so that the normal at the critical point is vertical. Around a stable node the gradient vector always points upwards. A saddle point partitions the surface into four quadrants, where the gradient vector's orientation alternates. In the vicinity of a mixed point comprising half a saddle and half a stable node the gradient points upwards in three quadrants, whereas with half an unstable node there is only one

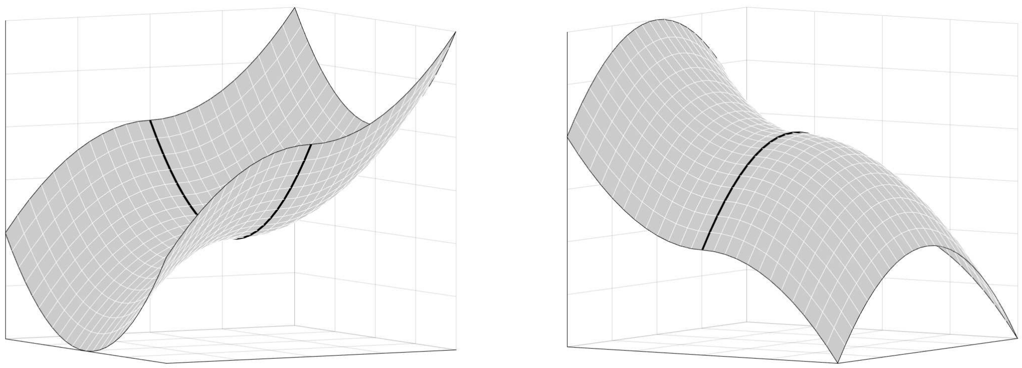

Figure 7: Saddle-node mixed critical point terrain: saddle-unstable-node and saddle-stable-node

such quadrant. Of course, near an unstable node there are no trajectories with an upward gradient. Thus the presence of mixed type critical points creates a continuous transition in the gradient vector orientation between a stable node and an unstable one. The emergence of mixed type critical points is directly related to the fact that the classical maximum principle for harmonic functions does not hold for the harmonic part of the anisotropic problem, and maxima or minima might be situated on the contiguity curves interior to the annulus boundary.

The existence of anisotropic solutions in other curvilinear coordinate systems is a topic of future study. Anisotropic solutions to other classical partial differential equations might also be of value, e.g. extending the theory developed herein to wave propagation in anisotropic media will be useful in modelling or quantifying of the viscoelastic properties of biological tissues [17].

Acknowledgement. The study was partly funded through the Thompson Rivers University undergraduate research apprenticeship programme.

Competing interests. The authors declare that they have no competing interests.

References

[1] Wise WR, Townsend TG. 2011 One-dimensional gas flow models for municipal solid waste landfills: cylindrical and spherical symmetries. *J. Environ. Eng.* **137(6)**, 514–516.

[2] Coats KH, Tek MR, Katz DL. 1959 Unsteady-state liquid flow through porous media having elliptic boundaries. *Petrol. Trans. AIME* **216**, 460–464.

[3] Adams KL, Russel WB, Rebenfeld L. 1988 Radial penetration of a viscous liquid into a planar anisotropic porous medium. *Int. J. Multiphase Flow* **14**, 203–215.

[4] Regan BD, Raynor PC. 2009 Single-fiber diffusion efficiency for elliptical fibers. *Aerosol Sci. Technol.* **43**, 533–543.

[5] Qian R, Shi J, Liu G, Pang B, Liu Z, She W, Zhang Y. 2021 Radial gas-permeability measurement in cement-based materials under steady-state flow. *Flow Meas. Instrum.* **79**, 101896.

[6] Hyman JD, Karra S, Makedonska N, Gable CW, Painter SL, Viswanathan HS. 2015 dfnworks: a discrete fracture network framework for modeling subsurface flow and transport. *Comp. Geosci.* **84**, 10–19.

[7] Germanou L, Ho MT, Zhang Y, Wu L. 2018 Intrinsic and apparent gas permeability of heterogeneous and anisotropic ultra-tight porous media. *J. Nat. Gas Sci. Eng.* **60**, 271–283.

[8] Lundegard PD, LaBrecque D. 1995 Air sparging in a sandy aquifer (Florence,Oregon, U.S.A.): actual and apparent radius of influence. *J. Contam. Hydrol.* **19**, 1–27.

[9] Morse P, Feshbach H. 1953 *Methods of theoretical physics.* McGraw Hill.

[10] Nec Y, Huculak G. 2020 Exact solutions to radial flow in a porous medium with variable permeability. *Phys. Fluids* **32**, 077108.

[11] Nec Y. 2021 Singularities in weakly compressible flow through a porous medium. *Fluid Dyn. Res.* **53**, 045507.

[12] Awasthi P, Kumar M, Nec Y. 2023 Anisotropic non-linear diffusion in spherical coordinates: flow patterns and transport efficiency. *SIAM J. Appl. Math.* **00**, 0.

[13] Gradshteyn IS, Ryzhik IM. 1980 *Table of integrals, series and products.* 4th edition, edited by Alan Jeffrey, Academic Press.

[14] GNU. 2021 *Octave, 6.2.0.* `https://www.gnu.org/software/octave/index`.

[15] Protter MH, Weinberger HF. 1984 *Maximum principles in differential equations.* Springer-Verlag.

[16] Kuzmin D, Shashkov MJ, Svyatskiy D. 2009 A constrained finite element method satisfying the discrete maximum principle for anisotropic diffusion problems. *J. Comput. Phys.* **228**, 3448–3463.

[17] Guidetti M, Royston TJ. 2018 Analytical solution for converging elliptic shear wave in a bounded transverse isotropic viscoelastic material with nonhomogeneous outer boundary. *J. Acoust. Soc. Am.* **144**, 2312–2323.